Journal of Physiology (2002), **541.3**, *pp.* 685–699
DOI: 10.1113/jphysiol.2001.015099
© The Physiological Society 2002
www.jphysiol.org

Rhythm generation in monkey motor cortex explored using pyramidal tract stimulation

A. Jackson, R. L. Spinks, T. C. B. Freeman, D. M. Wolpert and R. N. Lemon

Sobell Department of Motor Neuroscience and Movement Disorders, Institute of Neurology, University College London, London, UK

We investigated whether stimulation of the pyramidal tract (PT) could reset the phase of 15–30 Hz beta oscillations observed in the macaque motor cortex. We recorded local field potentials (LFPs) and multiple single-unit activity from two conscious macaque monkeys performing a precision grip task. EMG activity was also recorded from the second animal. Single PT stimuli were delivered during the hold period of the task, when oscillations in the LFP were most prominent. Stimulus-triggered averaging of the LFP showed a phase-locked oscillatory response to PT stimulation. Frequency domain analysis revealed two components within the response: a 15–30 Hz component, which represented resetting of on-going beta rhythms, and a lower frequency 10 Hz response. Only the higher frequency could be observed in the EMG activity, at stronger stimulus intensities than were required for resetting the cortical rhythm. Stimulation of the PT during movement elicited a greatly reduced oscillatory response. Analysis of single-unit discharge confirmed that PT stimulation was capable of resetting periodic activity in motor cortex. The firing patterns of pyramidal tract neurones (PTNs) and unidentified neurones exhibited successive cycles of suppression and facilitation, time locked to the stimulus. We conclude that PTN activity directly influences the generation of the 15–30 Hz rhythm. These PTNs facilitate EMG activity in upper limb muscles, contributing to corticomuscular coherence at this same frequency. Since the earliest oscillatory effect observed following stimulation was a suppression of firing, we speculate that inhibitory feedback may be the key mechanism generating such oscillations in the motor cortex.

(Received 4 December 2001; accepted after revision 5 April 2002)
Corresponding author R. N. Lemon: Sobell Department of Motor Neuroscience and Movement Disorders, Institute of Neurology, University College London, Queen Square, London WC1N 3BG, UK. Email: rlemon@ion.ucl.ac.uk

Oscillations in the motor cortex of monkeys and humans are dominated by activity in the 15–30 Hz or beta range (Murthy & Fetz, 1992, 1996; Sanes & Donoghue, 1993; Conway *et al.* 1995; Baker *et al.* 1997; Hari & Salenius, 1999). Baker *et al.* (1997) showed that, in a precision grip task, oscillations in macaque motor cortex were most pronounced during steady hold periods. Cortical local field potentials (LFPs) were coherent with muscle activity during this period, and we have suggested that these oscillations may help to maintain the motor set suitable for steady grip (Kilner *et al.* 1999, 2000).

In human subjects, coherence between cortex and muscle in the 15–30 Hz range has been demonstrated using electro- and magnetoencephalography (EEG and MEG) (Conway *et al.* 1995; Salenius *et al.* 1997; Halliday *et al.* 1998; Kilner *et al.* 1999). Generally, coherence is strongest with distal upper and lower limb muscles (Kilner *et al.* 2000; Mima *et al.* 2000). There is evidence that this coherence is mediated by the corticospinal tract, which has a particularly pronounced influence over distal limb function (Lemon, 1993). Previous studies have found phase lags between cortex and muscle that are consistent with conduction over the fast corticospinal pathway (Gross *et al.* 2000; Mima *et al.* 2000). Additionally, discharges of some primary motor cortex pyramidal tract neurones (PTNs) are phase locked, in the 15–30 Hz bandwidth, with the LFP oscillations (Baker *et al.* 1997; Pinches *et al.* 1997, 1999).

In defining the possible role of motor cortex PTNs in corticomuscular coherence, an important issue is whether they are subjected to oscillatory drive from an otherwise independent neural circuit or whether they form an integral part of that circuit. These alternatives are set out in a highly schematic manner in Fig. 1. PTNs could become phase locked to beta rhythms due to an oscillatory drive from a central oscillator (Fig. 1*A*) or their combined activity could influence the on-going rhythms (Fig. 1*B*), for example via collaterals at cortical or subcortical levels. To address this issue, we examined the effect on cortical oscillations of selectively exciting PTNs by stimulation of the medullary pyramidal tract (PT). If the rhythms are generated by circuitry independent of PTNs, then this stimulation should have no effect on the phase of the oscillatory cycle (Fig. 1*C*). However, if PTN activity influences rhythm generation, then synchronising these cells at an arbitrary time may interrupt the phase of the oscillatory cycle. Subsequent oscillations would be reset and have a consistent

Downloaded from jp.physoc.org by on March 23, 2008

phase relative to the stimulus, independent of when it was applied (Tass, 1999). In other words, the oscillation would become phase locked to the stimulus (Fig. 1*D*). A similar approach has been used to study other oscillatory networks (e.g. Perkel *et al.* 1964; Feldman *et al.* 1984; Ahmed, 2000; Staras *et al.* 2001).

This experiment was carried out in two macaque monkeys performing a precision grip task. We found significant phase-locked responses to PT stimulation in the LFP, single-unit and EMG activity, particularly in the 15–30 Hz frequency range, reflecting a resetting of natural on-going beta oscillations. We conclude that PTN activity directly influences the generation of 15–30 Hz rhythms.

Some of this work has been previously published in abstract form (Jackson *et al.* 2000).

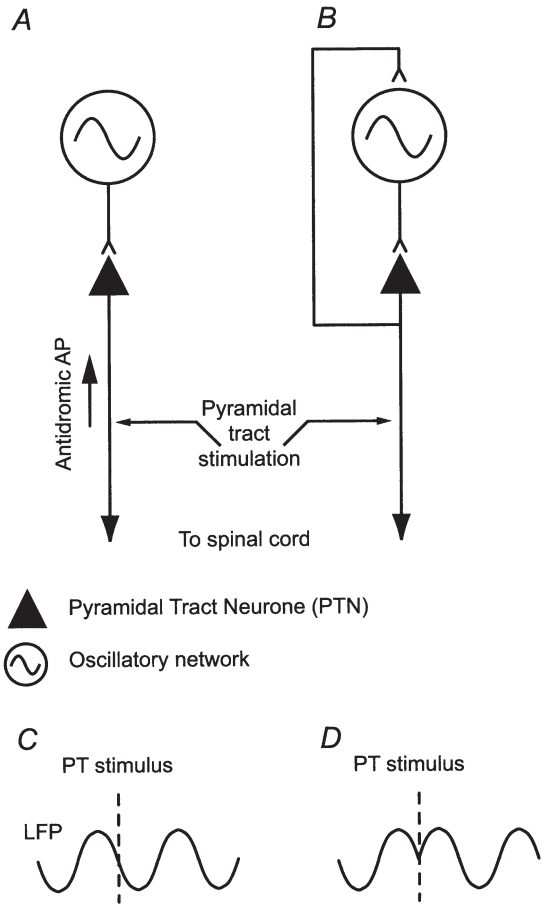

Figure 1. Highly schematic diagram of mechanisms for 15–30 Hz phase locking in motor cortex

Either the rhythm is generated by circuits independent of PTN activity, which drive the PTNs into phase with the rhythm (*A*), or the PTN activity is itself involved in the generation of the 15–30 Hz rhythm (*B*). These two possibilities are distinguished using pyramidal tract (PT) stimulation to set up antidromic action potentials (APs) in PTNs. If PTNs are not involved in generating the rhythm then the stimulus should have no effect on the phase of the oscillation (*C*). If PTNs lie within the rhythm-generating networks, then stimulation may reset the phase of on-going rhythms (*D*).

METHODS

Behavioural task

Two purpose-bred adult female macaque monkeys (M35 and M36; weights 5.1 and 5.0 kg, respectively) were trained to perform a precision grip task for food rewards (see Baker *et al.* 2001). This required squeezing two levers between the thumb and first finger of the left hand and holding within a position window for 1 s. Three auditory cues were given: the first indicated that the levers were within the target window; the second signalled that they had remained in target for at least 1 s; and the third occurred once the levers had been released and was accompanied by a fruit reward. The levers were mounted on the spindles of motors which were computer controlled to generate a spring-like force $F(x)$ of the form:

$$F(x) = kx + c, \quad (1)$$

where x is the lever displacement, the spring constant $k = 0.025$ N mm^{-1} (M35) or 0.04 N mm^{-1} (M36) and the constant $c = 0.15$ N. The target windows were 4–10 mm (M35) and 6–9 mm (M36).

Surgery

The animals were implanted under general anaesthesia (induced with 10 mg kg^{-1} ketamine I.M., maintained with 2–2.5% isoflurane in 50:50 O_2:N_2O) and aseptic conditions with a stainless-steel headpiece to allow head fixation. In a second operation, two varnish-insulated tungsten stimulating electrodes (impedance ~20 kΩ at 1 kHz) were implanted in the right medullary pyramid (stereotaxic co-ordinates A2.0, L1.5 and P3.0, L1.5; Snider & Lee, 1961), guided by a previous MRI scan (Baker *et al.* 1999). In M35, electrodes were also implanted at the same co-ordinates in the left pyramid (i.e. ipsilateral to the performing hand) and these were used for control purposes. Locations were confirmed during surgery by recording antidromic field potentials over motor cortex following stimulation. The thresholds for these potentials were 20 μA in M35 and 25 μA in M36. Postmortem histology confirmed the location of all electrode tips within the pyramids for both monkeys. Again aided by the MRI scan, a craniotomy was made and a circular chamber (i.d. 10 mm) positioned over the hand area of right primary motor cortex (stereotaxic co-ordinates for M35 were A10.8, L16.4; for M36 they were A10.0, L16.7).

During a further surgical procedure, monkey M36 was implanted with seven EMG patch electrodes (Miller *et al.* 1993) on the following muscles: first dorsal interosseous (1DI), abductor pollicis longus (AbPL), abductor pollicis brevis (AbPB), flexor digitorum superficialis (FDS), flexor digitorum profundis (FDP), extensor digitorum communis (EDC) and extensor carpi radialis-longus (ECR-L). All electrodes were led subcutaneously to a connector on the monkey's back.

After a period of recording in right hemisphere, M36 was retrained to perform the task with the right hand, and a new chamber was implanted over left primary motor cortex (A9.0, L18.0), along with corresponding PT and EMG electrodes.

All surgical operations were followed by a full course of antibiotic (20 mg kg^{-1} oxytetracycline I.M., Terramycin /LA, Pfizer Ltd) and analgesic (10 μg kg^{-1} buprenorphine I.M.,Vetergesic, Reckitt and Colman Products Ltd) treatment. At the end of the experiment, the animals were deeply sedated and then killed with an overdose of sodium pentobarbitone I.P. before perfusion through the heart. All procedures were carried out in accordance with UK Home Office regulations.

Downloaded from jp.physoc.org by on March 23, 2008

Recording

Details of the Eckhorn multiple-electrode recording system (Thomas Recording Ltd, Marburg, Germany) used for this study have been described elsewhere (Baker *et al.* 1999, 2001). Briefly, the drive allows a grid of glass-insulated platinum electrodes (impedance 1–3 MΩ, interelectrode spacing 300 μm) to be independently lowered into the cortex to search for cells and record the LFP. Typically between four and ten electrodes were used per session. PTNs were identified by their antidromic response to PT stimulation and collision testing (Lemon, 1984; Baker *et al.* 1999). Thresholds for antidromic identification were 10–200 μA. The signal from each recording electrode was amplified and then filtered for LFP (10–250 Hz) and spike activity (1–10 kHz). All data were recorded using a 32-channel digital tape recorder (RX832, TEAC). Sampling rates were 500 Hz and 24 kHz for LFP and spike data, respectively. EMG was amplified, high-pass filtered at 30 Hz (NL824, Neurolog, Digitimer, UK) and recorded at 24 kHz. Off-line, these data were rectified, smoothed and downsampled to 500 Hz.

Stimulation

PT stimuli consisted of biphasic constant current pulses (each phase 0.2 ms duration) delivered between the two PT electrodes. Single stimuli were delivered 0.5 s into the hold period (defined by both finger and thumb remaining within the target displacement) for 70 % of trials (M35) or 100 % of trials (M36). Additionally, in some sessions with M36, stimuli were delivered at the onset of movement, defined by finger or thumb lever displacement exceeding 1 mm. Current intensity was 150 μA in M35 and 10–100 μA in M36 (60 μA unless stated otherwise). Both the digital trigger pulse and current monitor waveform were recorded. After each recording session, localisation of the recording electrodes within the hand area of M1 was confirmed using intracortical microstimulation (ICMS; 13 biphasic pulses of width 0.2 ms, at 300 Hz). Thresholds for eliciting movement of the hand or digits (and EMG response in M36) were typically between 5 and 20 μA.

Analysis

Off-line, trials were accepted for analysis if two criteria were met: firstly, that the movement period (defined by finger or thumb velocity being greater than 30 mm s^{-1}) lasted less than 1 s; and secondly, that for the remainder of the trial both velocities were less than 30 mm s^{-1}.

LFP and EMG analysis. Phase locking of the LFP to the PT stimulus was determined using stimulus-triggered averaging of the unrectified recordings. For M36, similar analysis was also performed on the rectified EMG. Averages were compiled from 500 ms before to 500 ms after the stimulus. Although averaging in this way identifies clearly any phase-locked responses, no information is obtained about the frequency components within the time-locked signal. For this we used an analysis designed to quantify stimulus-locked power in the frequency domain. The calculation utilises the Fast Fourier Transform (FFT) algorithm on sections of data aligned to each stimulus of length L sample points. The Fourier coefficient $F_n(f)$ for the nth stimulus ($n = 1, 2, \ldots, N$) is a complex number representing the amplitude $a_n(f)$ and phase $\phi_n(f)$ of the component at frequency f:

$$F_n(f) = \frac{L}{2} a_n(f) e^{i\phi_n(f)}. \quad (2)$$

To compute the power spectrum $P(f)$, the squared magnitude of each coefficient is averaged across stimuli:

$$P(f) = \frac{1}{N}\sum_{n=1}^{N}\left|\frac{2}{L}F_n(f)\right|^2 = \frac{1}{N}\sum_{n=1}^{N} a_n(f)^2. \quad (3)$$

Stimulus-locked power $P_{s\text{-}l}(f)$ is calculated by instead averaging the coefficients *before* taking the squared magnitude:

$$P_{s\text{-}l}(f) = \left|\frac{1}{N}\sum_{n=1}^{N}\frac{2}{L}F_n(f)\right|^2. \quad (4)$$

In this way, the phase of each data section is incorporated within the average. Components without a constant phase relative to the stimulus will average out, leaving only that part of the signal which is phase locked. Note, however, that in contrast to the method of 'phase-averaging' (Jervis *et al.* 1983; Tallon-Baudry *et al.* 1996), the amplitude of each component is still incorporated within the stimulus-locked power spectrum. Both total and stimulus-locked power spectra were calculated for a 128 sample point (256 ms) rectangular window from 2 to 258 ms after the stimulus and compared with an equivalent window from 258 to 2 ms before the stimulus (avoiding any stimulus artefact). In addition, time–frequency plots were obtained using a 128 point window sliding through the data in 40 ms steps.

It should be noted that the stimulus-locked power analysis is equivalent to existing methods for separating phase-locked and non-phase-locked components of a signal in the time domain based on intertrial variance (Kalcher & Pfurtscheller, 1995). However, the frequency domain calculation has several advantages for this study. Firstly, information about the entire frequency spectrum is readily obtained. Secondly, it is possible to test the statistical significance of phase locking. This is important since no measure of the phase-locked component of a signal will exactly equal zero. Even with no consistent phase relative to the stimulus, there will be residual noise after averaging. Previous methods have used a period before the stimulus as a baseline with which to compare the evoked response (Pfurtscheller & Lopes da Silva, 1999). However, if the total power in the signal increases after the stimulus, there may be a corresponding increase in the noise component. In comparison with the baseline, this might then be mistakenly interpreted as a significant phase-locked signal. Instead, we tested the significance of stimulus-locked power by comparison with stimulus-locked power calculated from the same sections of post-stimulus data which were then phase shifted randomly. These simulated data therefore had the same distribution of amplitudes as the real data, but no consistent phase relative to the stimulus. Repeated calculation for different sets of simulated data yielded the expected distribution of stimulus-locked power in the absence of phase resetting, from which the ninety-fifth centile was calculated. Values greater than this were then considered evidence of a significant phase-locked effect at the 95 % confidence level. In some cases, we calculated the equivalent P value for rejecting the null hypothesis of no consistent phase relationship between the signal and the stimulus. Note that this method differs from statistical tests of phase distribution (e.g. Sayers & Beagley, 1974; Jervis *et al.* 1983) in that it takes into account the amplitude distribution of the Fourier coefficients.

Results from data recorded from individual electrodes for each session were combined into histograms of the frequencies of peak stimulus-locked power. So that results were not biased towards sessions in which more electrodes were used, the contribution of

Downloaded from jp.physoc.org by on March 23, 2008

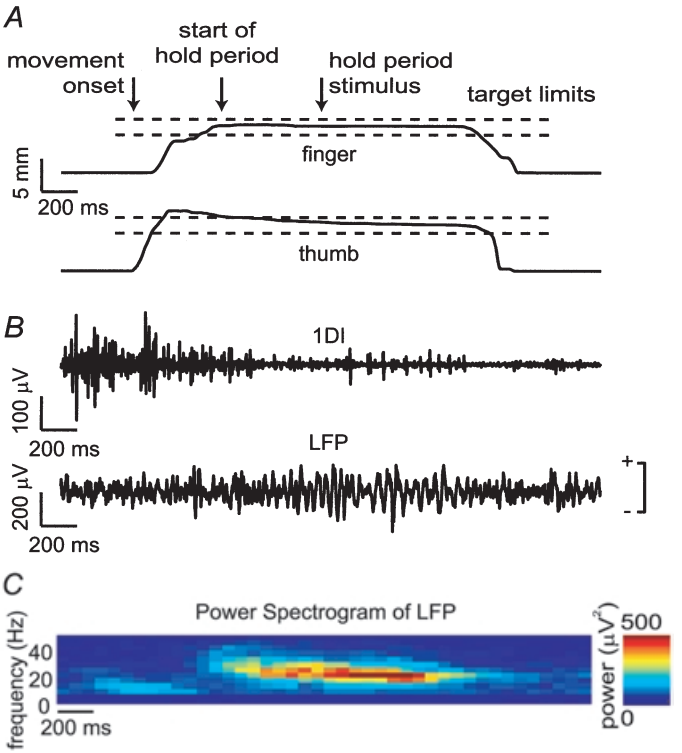

Figure 2. Local field potential oscillations during precision grip task

A, finger and thumb position traces for a successful control trial (M36) performed with the left hand; horizontal dashed lines indicate the target displacement windows. Arrows show movement onset, beginning of hold period and time of the PT stimulus (not actually delivered during this trial). *B*, EMG recorded from the left 1DI muscle and local field potential (LFP) recorded from an electrode in the right M1 during the same trial. Polarity of this and subsequent LFP recordings is indicated. *C*, power spectrogram of LFP averaged over 50 control trials (no stimulation) showing power in the beta frequency range during the hold period of the task.

each electrode towards the histograms was weighted inversely to the number of electrodes used in that session.

Spike data analysis. Single units were discriminated off-line using principal component analysis on the spike waveform and cluster cutting (Baker *et al.* 1999). Normalised autocorrelograms were used to assess periodic firing patterns (Abeles, 1982). Peri-stimulus time histograms (PSTHs), also normalised into units of spikes s^{-1}, were compiled between 200 ms before and after the stimulus, with a bin width of 5 ms. The average bin count for the prestimulus period was calculated. Post-stimulus bins with counts outside the

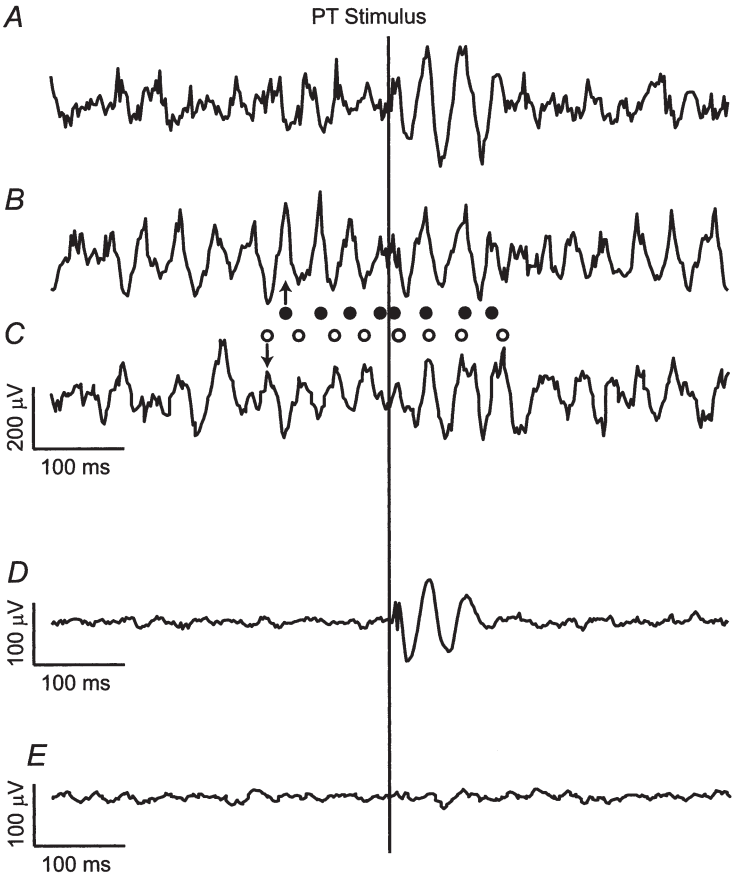

Figure 3. Stimulus-triggered averages of LFP

A, *B* and *C*, sample traces of LFP aligned to the PT stimulus, recorded during three different trials (150 μA; monkey M35). Single stimuli were delivered to the PT ipsilateral to the recording site during the hold period. Note that a complex wave was evoked by the PT shock, irrespective of whether there was on-going oscillatory activity before the stimulus (*B* and *C*) or not (*A*). Resetting of the on-going activity is demonstrated by rhythmic activity in traces *B* and *C* being out of phase before the stimulus, but in phase after it (filled circles indicate peaks of trace *B*, open circles indicate peaks of trace *C*). *D*, average of 110 traces shows phase locking of LFP for 100–150 ms after the stimulus. *E*, stimulus-triggered average for contralateral PT stimulation (150 μA, 110 trials) showed no effect.

Downloaded from jp.physoc.org by on March 23, 2008

95 % central range (calculated from a Poisson distribution) were considered significant.

RESULTS

Database

Analysis in this paper is based on 25 recording sessions (12 for M35 and 13 for M36) in the hand representation of the primary motor cortex (M1), in all cases contralateral to the performing hand. Results obtained with PT stimulation in the hold period were recorded from the right hemisphere. Following retraining with the right hand, three sessions with M36 were recorded from the left hemisphere for PT stimuli delivered during both the movement and the hold period. Most of the LFP and single-neurone recordings were made in the anterior bank of the central sulcus. A total of 65 neurones were analysed (29 and 36 neurones from the right hemispheres of M35 and M36, respectively). Of these, 42 (65 %) were identified as PTNs, with antidromic latencies ranging from 0.9 to 4 ms; most had short

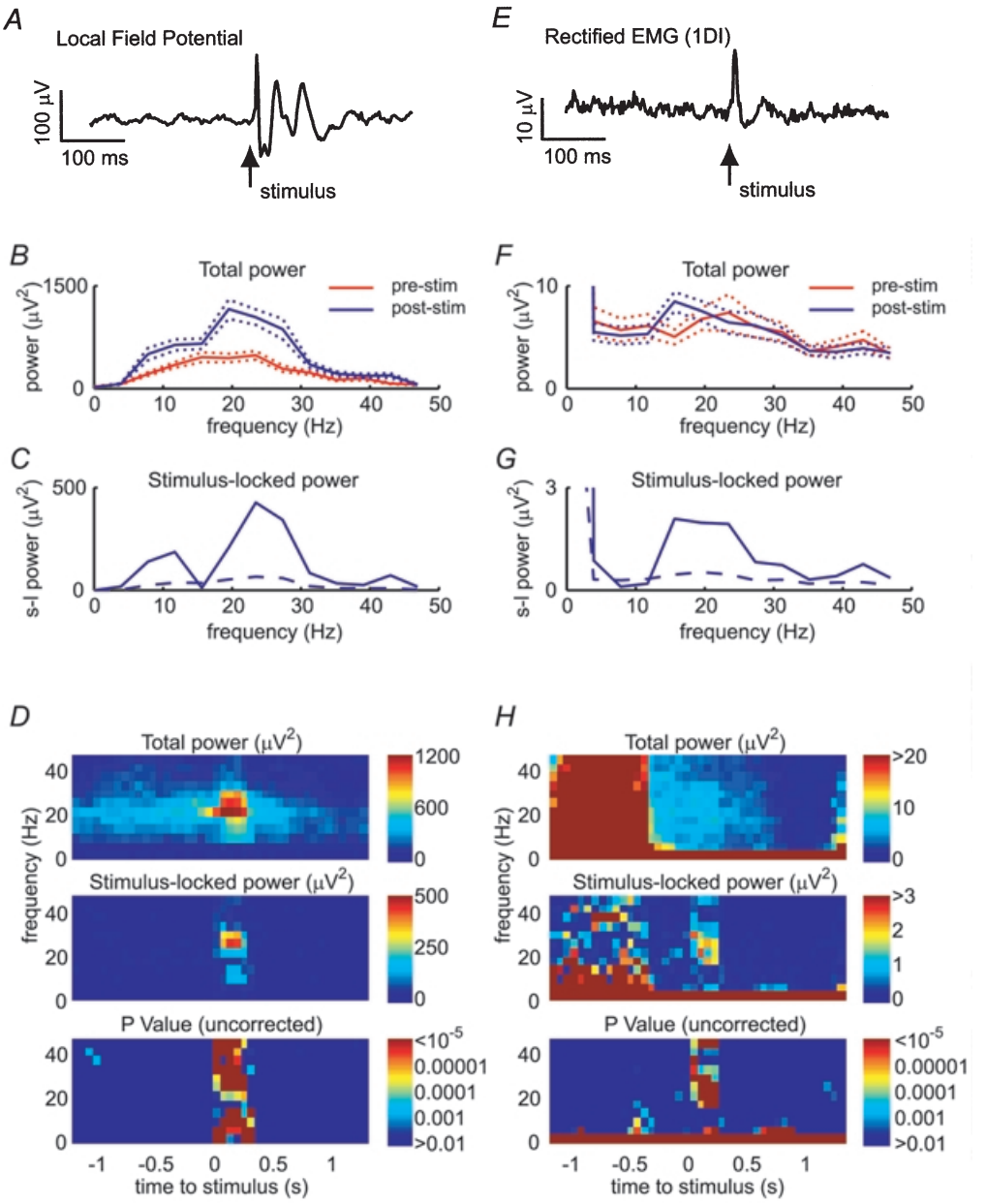

Figure 4. Frequency domain analysis of phase resetting of LFP and EMG

A, stimulus-triggered average of LFP (M36, 50 trials, 60 μA). *B*, power spectra for 256 ms prestimulus and post-stimulus periods. *C*, stimulus-locked power spectrum for post-stimulus period. Dashed line represents ninety-fifth centile (corresponding to significant phase locking at 95 % level) obtained from phase-shifted data (see Methods). *D*, time–frequency spectrograms of power and stimulus-locked power with equivalent *P* values. *E–H*, equivalent analysis performed on rectified EMG recorded from 1DI during the same period as *A–D*.

Downloaded from jp.physoc.org by on March 23, 2008

latencies (<1.5 ms). Sixteen neurones in M36 were further identified by spike-triggered averaging of EMG as cortico-motoneuronal (CM) cells (Buys *et al.* 1986).

Beta oscillations during the hold period of the precision grip task

Figure 2*A* shows finger and thumb position traces from a single trial (without PT stimulation). The hold period was defined as the time during which both finger and thumb remained inside the target windows defined by dashed lines. Corresponding EMG and LFP recordings for this trial are shown in Fig. 2*B*. Oscillatory activity is evident in the LFP trace during the hold period. Figure 2*C* shows a time–frequency plot of LFP power averaged over 50 trials, aligned to the start of the hold period. As has been reported previously (Baker *et al.* 1997), power is observed in the 15–30 Hz band for the duration of the hold, but not during the movement phases.

Effect of PT stimulus (time domain)

Figure 3*A*, *B* and *C* shows sweeps of LFP data from three different trials recorded during the same session from one M1 electrode site. In all cases a PT stimulus (150 μA) was delivered 500 ms into the hold period as indicated. It is clear from these traces that the degree of on-going oscillatory activity varied between trials. For the trial shown in Fig. 3*A*, where oscillatory activity before the stimulus was less clear, PT stimulation evoked a response consisting of three cycles at around 25 Hz. In the trials shown in Fig. 3*B* and *C*, rhythmical activity in the LFP at this same frequency was pronounced both before and after the stimulus. However, resetting of the oscillation by the PT stimulus is indicated by the phase of the cycles immediately following the stimulus. In all three cases, the LFP oscillated with the same relative phase for around 100 ms after the stimulus. Phase resetting is confirmed by comparison of Fig. 3*B* and *C*. In the period immediately before the stimulus the oscillations were out of phase (circles on the left of the stimulus line), whereas afterwards they were clearly in phase (circles on the right). Since single sweeps are inherently noisy, more convincing evidence for phase resetting is provided by stimulus-triggered averages. Figure 3*D* shows an average of 110 trials aligned to the stimulus. The phase-locked response began 2–10 ms after the stimulus with a peak amplitude in this case of around 200–300 μV in single trials (Fig. 3*A*), reduced to around 100 μV in the average (Fig. 3*D*). That this phase-locked oscillation disappears from the average after two to three cycles probably reflects the variability in the oscillation frequency across trials. Examination of Fig. 3*B* and *C* shows the reset oscillation persisting in single trials. Figure 3*E* shows a stimulus-triggered average recorded from the same electrode when stimuli (150 μA) were delivered to the opposite pyramid (contralateral to recording site). No phase-locked oscillatory response was evoked from this side (4 recording sessions).

Effect of PT stimulus (frequency domain)

Frequency domain analysis of LFP and EMG data (Fig. 4) shows how the frequency components of the reset response were related to the on-going oscillatory activity. Stimulus-triggered averages (Fig. 4*A* and *E*) suggest phase-locked responses in both LFP and rectified EMG following a PT stimulus of 60 μA during the hold period. The power spectrum of the prestimulus LFP (Fig. 4*B*) showed a broad peak in the 15–30 Hz bandwidth, which was enhanced following stimulation. This increase is to be expected given the presence of trials where stimulation excited rather than reset oscillation (see Fig. 3*A*). Figure 4*C* shows the stimulus-locked power spectrum for the post-stimulus LFP (see Methods). There was a significant peak at 23 Hz, the same frequency as the prestimulus oscillation, suggesting the phase of this rhythm had been reset. There was also a phase-locked component around 10 Hz. The presence of

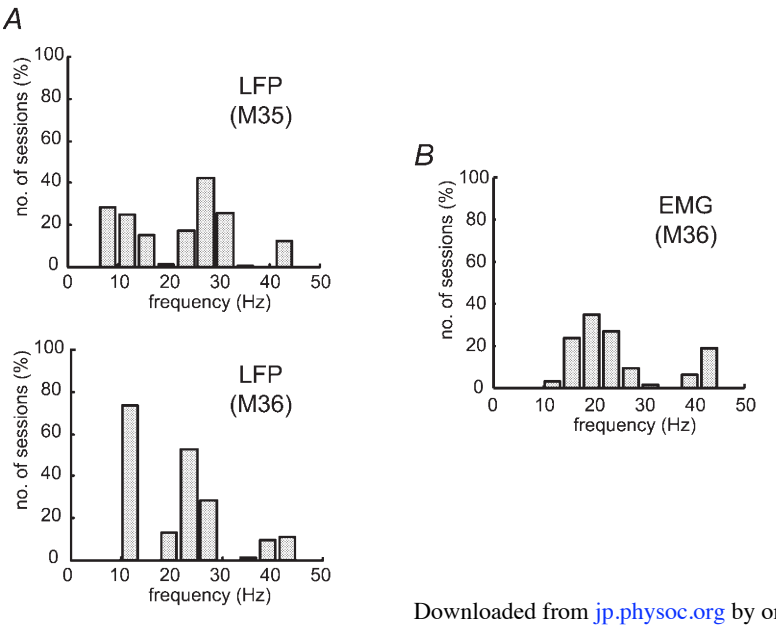

Figure 5. Frequencies of peak stimulus-locked power in LFP and EMG

A, histogram showing frequencies of significant peaks in stimulus-locked LFP power spectra. Note bimodal distribution of phase-locked response. *B*, frequencies of significant peaks in stimulus-locked EMG power spectra (M36; all muscles pooled). No phase-locked response at 10 Hz was observed in the EMG activity.

Downloaded from jp.physoc.org by on March 23, 2008

this lower frequency in around 70 % of sessions is interesting since there was no peak at this frequency in the power spectrum of the prestimulation recording; it represents a second oscillatory component excited by PT stimulation. Figure 4*D* shows time–frequency plots of these power changes using a sliding window through 1.5 s either side of the stimulus, along with the equivalent *P* value for significant phase locking.

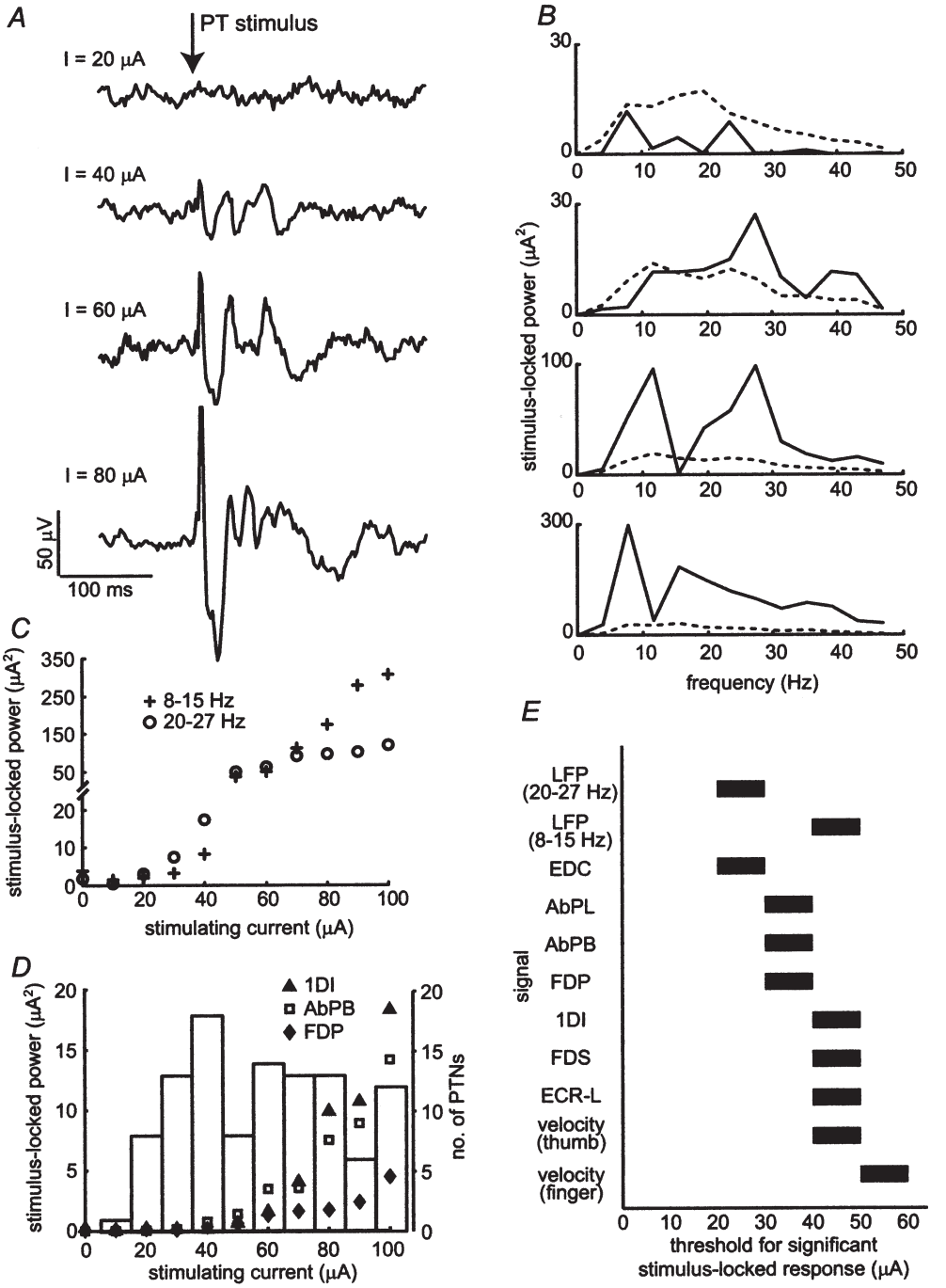

Figure 6. Effect of PT stimulation intensity

A, comparison of stimulus-triggered averages of LFP at different PT stimulation intensities (M36, 50 trials per intensity). *B*, corresponding stimulus-locked LFP power spectra. *C*, stimulus-locked LFP power averaged over the 8–15 Hz band and the 20–27 Hz band for different stimulation intensities (50 trials per intensity). *D*, stimulus-locked EMG power (averaged over the 17–24 Hz band) for activity from three muscles plotted against stimulation intensity. Overlaid is a histogram of antidromic thresholds up to 100 μA for a large sample of PTNs recorded from M36. Data from 150 PTNs in total; only a subset of these were collected for this study. *E*, thresholds for significant stimulus-locked power (at 95 % confidence) for LFP, EMG and velocity recordings. For example, a bar between 40 and 50 μA indicates that significant stimulus-locked power was observed with a stimulating current of 50 but not 40 μA.

Downloaded from jp.physoc.org by on March 23, 2008

Equivalent analysis was performed on the rectified EMG recorded from 1DI (Fig. 4*E–H*). This had a relatively flat power spectrum before stimulation, with little overall increase in the post-stimulus period (Fig. 4*F*). However, the stimulus-locked power spectrum for the post-stimulus period showed a single peak around 20 Hz (Fig. 4*G*). This is consistent with oscillatory activity being reset without an overall increase in amplitude. Note that, in contrast to the LFP data, there was no lower frequency component around 10 Hz in the stimulus-locked power spectrum.

Figure 4 also demonstrates one of the advantages of the stimulus-locked power method for assessing phase resetting. Due to the increased EMG activity during the movement phase, there was a corresponding increase in the background level of stimulus-locked power at all frequencies between 0.5 and 1 s before the stimulus (Fig. 4*H*). However, the *P* values calculated from the phase-shifted data, as described in the Methods, show that this does not represent significant phase locking to the stimulus. The remaining low-frequency stimulus-locked effects are genuine and reflect task modulation of EMG activity.

Figure 5 shows histograms of the frequencies of significant peaks in the stimulus-locked power spectra, compiled for all sessions in the two animals. A bimodal distribution is evident for the LFP, with one component around 10 Hz and a higher frequency component around 23–27 Hz (Fig. 5*A*). Significant phase resetting was observed both on electrodes which were simultaneously recording spike activity and on electrodes devoid of spikes. Thus, these effects are not the result of incomplete filtering of spike waveforms from the LFP. For the EMG, there was no lower frequency component (Fig. 5*B*). Note that the peak frequency observed in the EMG response appears to be slightly lower than in the LFP (see Discussion). A small but significant phase locking effect occurred at around 40 Hz in both LFP and EMG in around 25 % of sessions (cf. Fig. 4).

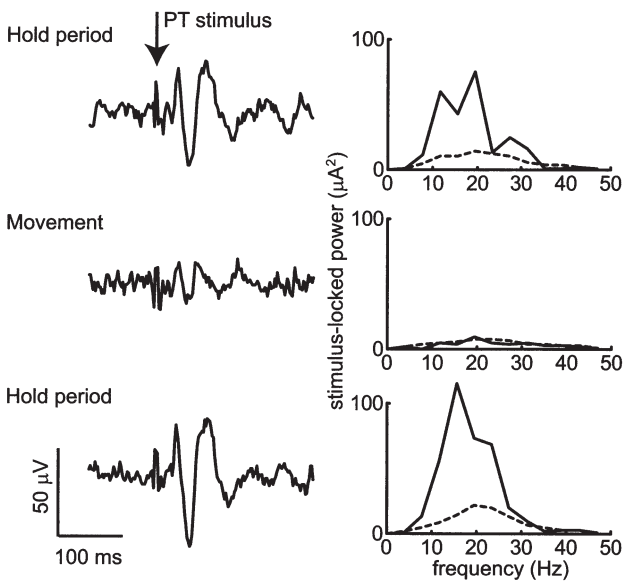

Figure 7. Comparison of resetting effects during movement phase and hold period

Stimulus-triggered LFP averages and corresponding stimulus-locked power spectra for 100 stimuli delivered during the hold period, followed by 100 stimuli at movement onset, then a repeat of 100 during the hold period. The oscillatory response was greatly reduced when stimuli were delivered at movement onset. These recordings were made from the left hemisphere of M36 with a stimulating current of 100 μA.

Effect of stimulus intensity

Figure 6*A* shows averaged LFP for PT stimulation with intensities between 20 and 80 μA. The response at higher currents was larger and had a different frequency composition, as indicated in Fig. 6*B*. With a current of 40 μA, the only significant phase-locked effect was at around 25 Hz. As the stimulating current was increased, a 10 Hz component appeared and increasingly dominated the response. This differential increase, shown in Fig. 6*C*, suggests that these two frequencies may have arisen from different neuronal mechanisms or circuits (see Discussion). The currents required to reset cortical oscillations are relatively low compared to the antidromic thresholds for most PTNs recorded in this animal (Fig. 6*D*). A current of 40 μA was sufficient to antidromically activate 25 % of the PTNs identified in this animal (M36). That this current induced observable effects in the LFP suggests that synchronisation of a subset of PTNs by the stimulus had an influence on the larger population of cells, and this was confirmed by the single-unit results (see next section). The intensity-related increase in stimulus-locked EMG power is overlain on Fig. 6*D* for EMG recordings from three muscles.

The bars in Fig. 6*E* show the thresholds for eliciting a significant stimulus-locked power (above the 95 % confidence level) in the LFP, EMG and lever velocities. Phase locking to the PT stimulus first appeared in the cortical LFP (20–27 Hz band) at 30 μA and this was followed by responses in the EMG between 30 and 50 μA. Phase locking of the LFP in the 8–15 Hz band appeared at 50 μA. Finally, a small movement response, detected from equivalent analysis of the lever velocity signals, was observed at 50–60 μA.

Effect of PT stimuli during the movement phase

Figure 7 compares the LFP response to PT stimulation during the hold and movement periods of the task. Averages of LFP are shown for consecutive delivery of 100 hold period stimuli, then 100 movement stimuli, followed by a repeat of 100 hold period stimuli. As can be seen, the phase-locked response to stimulation was greatly reduced during movement, corresponding to the period when spontaneous oscillations were absent from the LFP (see Fig. 2*C*).

Downloaded from jp.physoc.org by on March 23, 2008

Effect of delivering PT stimuli on periodic firing of single PTNs

A further demonstration of the capacity of PT stimulation to effectively reset on-going oscillatory activity during the hold period was obtained by examining the discharge of single, antidromically identified PTNs. Many PTNs exhibit regular spike patterns during the hold period, which are known to be in phase with the LFP (Baker *et al.* 1997). Subsequently, if PT stimulation resets oscillations observed in the LFP, it should also reset the rhythmical firing of

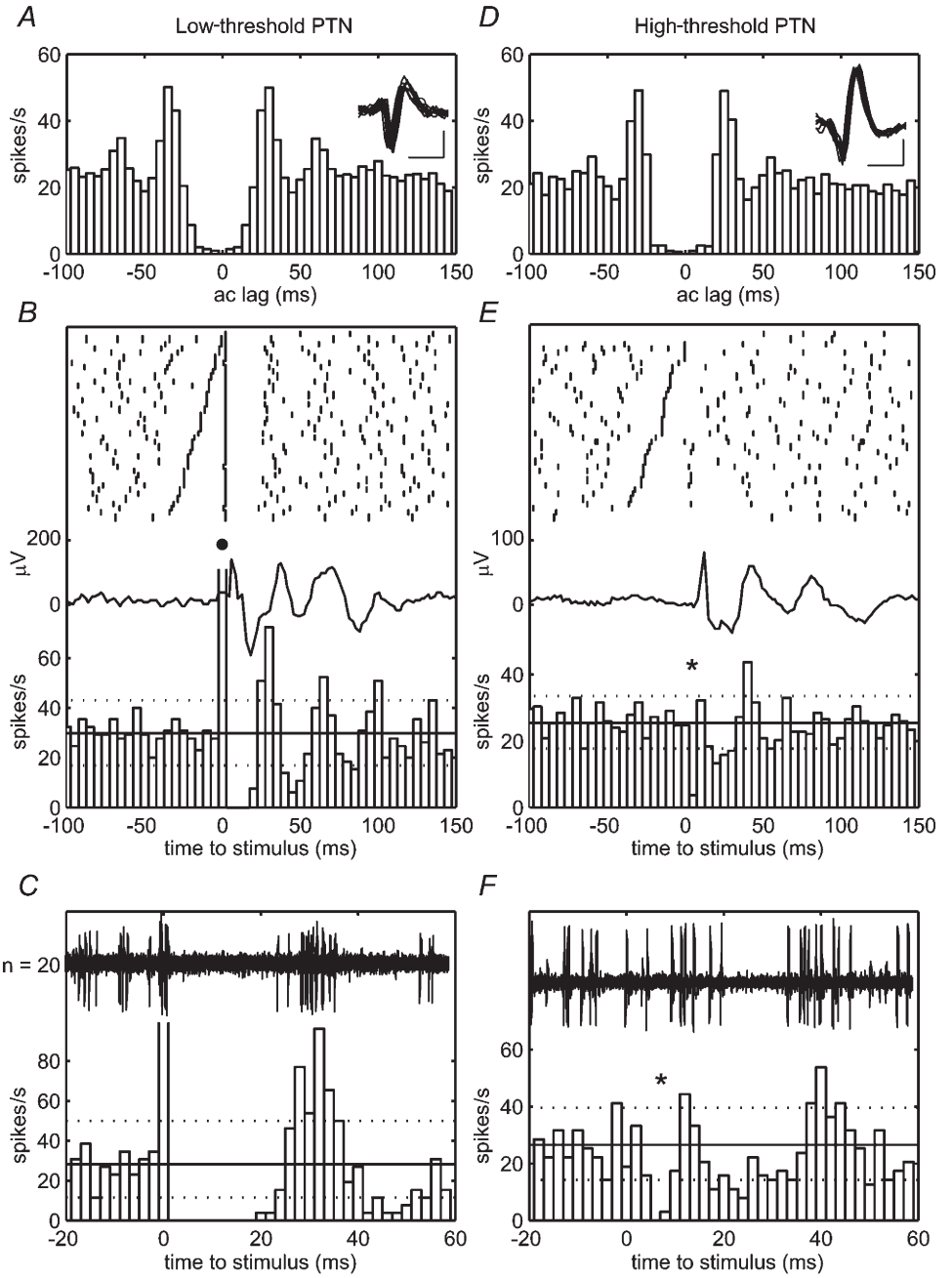

Figure 8. Resetting of motor cortex single-unit activity

A, normalised autocorrelogram and overlain waveforms of 10 spikes of an oscillatory PTN (M35) compiled from spikes occurring during the hold period (75 trials). Calibration bars, 500 μs, 50 μV. *B*, raster plots and normalised PSTH for the same cell with reference to the PT stimulus (150 μA). This PTN exhibited an antidromic response to the PT stimulus (●) so was classed as low threshold. Subsequent firing was rhythmical and time locked to the stimulus and the reset LFP average (overlain). *C*, expanded view of antidromic response and subsequent initial period of suppression which lasted for around 20 ms. Overlain are 20 single sweeps of raw data. *D*, normalised autocorrelogram for high-threshold oscillatory PTN (M36, 100 trials). *E*, PSTH reveals phasic suppression and facilitation following stimulation (60 μA). *F*, expanded view showing short-latency suppression following stimulus (*). Dotted lines represent 95% central range around mean firing rate.

Downloaded from jp.physoc.org by on March 23, 2008

PTNs. For the purposes of this analysis PTNs were classed as either 'low threshold' if the stimulus intensity used evoked an antidromic response, or 'high threshold' if an antidromic response could only be elicited at higher intensities. Note that these terms are relative to the stimulus strength used in each animal. Thus, a greater proportion of cells in monkey M35 were classed as low threshold because a higher stimulus strength was used in this animal (150 μA in M35 and 60 μA in M36). In addition, cells for which no antidromic response could be elicited with currents up to 200 μA were classed as unidentified (UID).

Figure 8*A* shows the normalised autocorrelogram for a PTN recorded from monkey M35. The autocorrelogram was compiled from spikes occurring during the hold period of the task. Regular peaks at 30 ms and 60 ms lags indicate rhythmical discharge at around 30 Hz. Figure 8*B* shows raster plots aligned to the stimulus and the PSTH for this cell. The threshold for antidromic excitation of this cell was 40 μA. It was classed as low threshold since the stimulation at 150 μA discharged the neurone on almost every occasion (●); the exceptions were due to a small number of collisions with orthodromic spikes. Each antidromic spike occurred at a short, constant latency and was followed by a period of around 20 ms during which there was a complete suppression of spontaneous discharge (Fig. 8*C*). The neurone then resumed firing in periodic fashion time locked to the stimulus, as indicated by peaks in the PSTH. These occur in phase with the oscillations in the averaged LFP, which was recorded simultaneously and is overlain in Fig. 8*B*. Thus there is clear evidence on a single-unit level that PT stimulation could reset oscillatory activity in the motor cortex.

The PTN shown in Fig. 8*D–F* was classified as high threshold since stimulation (60 μA, monkey M36) did not elicit an antidromic response. The threshold for antidromic excitation of this cell was 150 μA. However, the cell was clearly affected by the stimulus because there was a short-latency suppression of on-going activity (marked by * in Fig. 8*E* and expanded in Fig. 8*F*). This was not the result of stimulus artefacts interfering with discrimination of the spikes. Examination of Fig. 8*F* shows that suppression began 4 ms after the stimulus and lasted for a further 4 ms; the brief stimulus artefact lasted less than 1 ms. There was then a second period of suppression between 15 and 30 ms, followed by a period of increased discharge at 40 ms. The timing of these effects relative to the stimulus corresponds to the reset beta rhythm (see average of LFP in Fig. 8*E*).

Figure 9 summarises all the latencies following PT stimulation at which significant facilitation or suppression was observed in PSTHs of single neurones. A total of 65 neurones were analysed, of which 53 (82 %) exhibited significant modulation of discharge following stimulation.

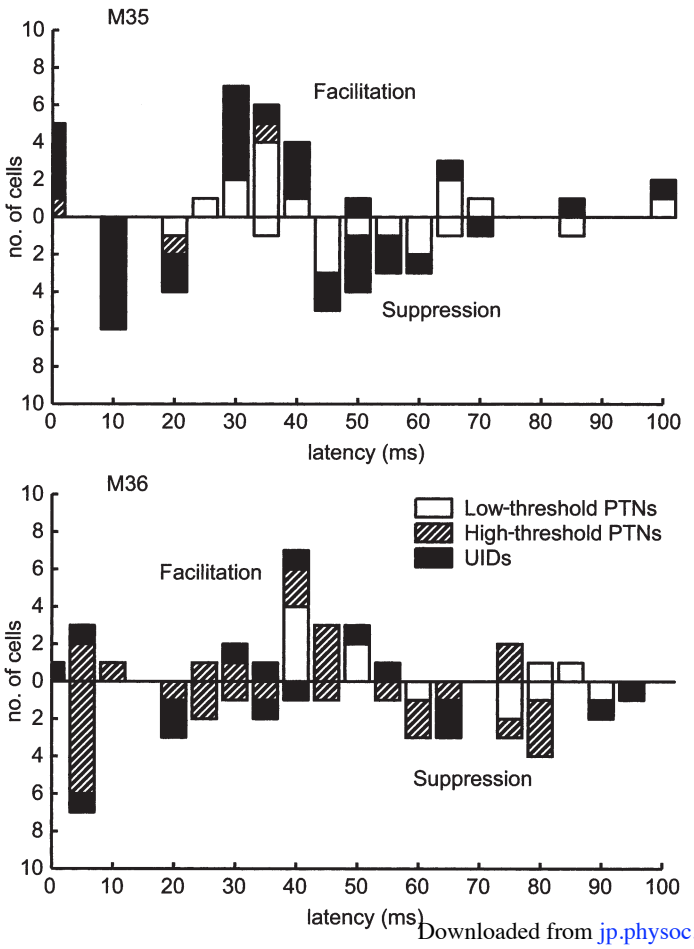

Figure 9. Summary of PT-evoked suppression and facilitation

Histograms showing latencies of significant peak facilitation (upwards bars) and suppression (downwards bars) following PT stimulation. Effects were tested at 95 % confidence level. Short-latency effects were mainly inhibitory. At longer latencies (30–50 ms) there was facilitation of most cells irrespective of whether an antidromic response was elicited. This reflects a synchronisation of cell firing in the 15–30 Hz range. Data based on a total of 65 cells, 53 of which exhibited significant modulation of firing in the 100 ms following the PT stimulus.

Downloaded from jp.physoc.org by on March 23, 2008

As can be seen, most of the short-latency effects (< 20 ms) were inhibitory. At longer latencies (30–45 ms), responses in all cell categories were mainly facilitatory, and in the period from 45 to 65 ms, suppression dominated once again. These phasic periods of suppression and facilitation reflect the synchronisation of the units in the 15–30 Hz frequency range. There was no qualitative difference between the distributions of these effects for the cell types analysed. Low- and high-threshold PTNs with both short and longer latencies were reset in this way. Even cells which could not be antidromically excited (UIDs) became entrained to the PT stimulus. This may explain why significant stimulus-locked LFP could be evoked by the activation of a relatively small proportion of PTNs. Furthermore, since the first effect was one of suppression, this suggests a role for inhibition in imposing this oscillatory synchrony between PTNs (see Discussion).

DISCUSSION

PTNs and oscillatory networks

We have shown that stimulation of the pyramidal tract resets the phase of 15–30 Hz oscillations observed in the motor cortex. This result indicates that the PTNs must either be incorporated into or have a direct effect upon the networks producing these oscillations, and rules out the possibility that the rhythms arise from separate networks projecting to PTNs. Our findings provide further evidence for a link between 15–30 Hz oscillations and corticospinal function, as suggested by Baker *et al.* (1997). Furthermore, we have shown that the first rhythmical effect of stimulation after the antidromic response is a suppression of PTN firing. A number of experimental and modelling studies (Lytton & Seynowski, 1991; Whittington *et al.* 1995, 2000; Pauluis *et al.* 1999) have implicated inhibitory interneurones in the generation of oscillations. Widespread inhibition within a neuronal network is a probable source of synchrony, characterised by synchronised discharge as neurones emerge from the inhibitory state (Lytton & Sejnowski, 1991). The timing of synchrony is dependent both on the intrinsic properties of the inhibitory interneurones and their conduction delays (Pauluis *et al.* 1999). In human subjects, transcranial magnetic stimulation (TMS) over the motor cortex is known to induce a silent period in muscles, which may be partly due to a disfacilitation of corticospinal inputs (Kujirai *et al.* 1993). This is followed by a period of increased motor unit coherence (Mills & Schubert, 1995). In this context, it is interesting to note that TMS has been shown to reset both involuntary tremor (Britton *et al.* 1993) and voluntary rhythmical movements (Wagener & Colebatch, 1996). Our finding of a period of suppression up to 30 ms post-stimulus is consistent with the hypothesis that inhibitory feedback could be responsible for synchronising PTNs and entraining them to the 15–30 Hz rhythm.

The pathway through which this inhibitory feedback arises remains uncertain. Firstly, it is clear that this is specific to the ipsilateral pyramidal tract, since no resetting was observed with stimulation of the contralateral tract (Fig. 3*E*). The effects we have observed could result from either orthodromic or antidromic activation of PT axons. It seems unlikely that the effects are due to stimulation of other nearby structures (for example, the medial lemniscus) because the tips of the electrodes were located within the PT, and phase resetting of LFP oscillations was observed with very low currents (< 50 μA).

Orthodromic impulses. One possibility is that the resetting results from reafferent inputs generated by the muscle twitches produced by descending corticospinal volleys. Thus, the circuit generating the beta oscillations would consist of a closed loop from motor cortex to muscle, returning via afferent inputs. Although it is known that stimulation of these afferents can produce event-related synchronisation (Salmelin & Hari, 1994; Salenius *et al.* 1997), this occurs at much longer latencies than found here and only after an initial period of desynchronisation. Subsequent oscillations are not phase locked to the stimulus. Furthermore, the thresholds for EMG and motor responses in our study were generally higher than for phase locking of the LFP (Fig. 6*E*). Finally, the relatively long delays between the onset of a motor response and the time of arrival of reafferent inputs to motor cortex exclude such mechanisms from contributing to at least the earliest effects observed in Fig. 8. However, resetting could still result from changes in the transmission of afferent inputs that is under descending corticospinal control; many PT axons terminate in the dorsal column nuclei and spinal dorsal horn (Kuypers, 1981; see Porter & Lemon, 1993).

Antidromic impulses. A more likely mechanism underlying the effects observed would be the antidromic invasion of intracortical collateral branching from PTNs (Landry *et al.* 1980; Ghosh & Porter, 1988; Huntley & Jones, 1991). Large pyramidal neurones, similar to those giving rise to the PT, typically generate three to five collaterals (Ghosh & Porter, 1988; Abeles, 1991), which arborise mostly in lamina V and VI. These collaterals provide inputs to a number of different targets, including other pyramidal neurones (Renaud & Kelly, 1974*b*; Kang *et al.* 1991; Baker *et al.* 1998) and a variety of intracortical inhibitory interneurones (Renaud & Kelly, 1974*a*; Thomson *et al.* 1995; Thomson *et al.* 1996; Thomson & Deuchars, 1997). In visual cortex, inhibitory interneurones are thought to account for 2–10 % of pyramidal axon targets (Thomson & Deuchars, 1997). These interneurones in turn can exert powerful inhibition of pyramidal neurones in their immediate vicinity (DeFelipe *et al.* 1985; Kisvarday *et al.* 1990; Thomson *et al.* 1996) and are a likely source of the profound suppression of PTN discharge seen at relatively short latency (<10 ms) after PT stimulation (Figs 8 and 9).

Downloaded from jp.physoc.org by on March 23, 2008

The longer latency suppression (15–30 ms) could result from activation of corticothalamic loops, a well-known source of oscillatory activity (Steriade, 1999; Marsden *et al.* 2000). In addition, subcortical collaterals of corticospinal axons, such as those which terminate in the pontine nuclei (Ugolini & Kuypers, 1986) could influence cerebellar activity. It is known that cerebellar damage can interfere with beta rhythms (Pohja *et al.* 2000) and reciprocal connections between motor cortex and lateral cerebellum (Holdefer *et al.* 1999, 2000) may underlie movement-related oscillatory activity in the cerebellum (Pellerin & Lamarre, 1997).

If it is the antidromic impulse which resets the cortical rhythm, then this may explain why a slightly lower frequency of evoked oscillatory activity is observed in the EMG compared with that in the cortical LFP. This is due to the complicating effects of the short-latency EMG response to the orthodromic action potentials set up by PT stimulation. This will occur slightly earlier than the first oscillatory burst of descending activity once the antidromic PT impulses have reached the cortex and reset the beta rhythms. Thus the first oscillatory cycle observed in the muscle will be slightly longer than the corresponding cortical period; it will be extended by the conduction time from the pyramid to cortex and back again. This time can be estimated from the sum of the antidromic latency and the collision interval of the PTNs. For M36, this sum was typically in the range of 1–6 ms. The increased time period would lead to a corresponding frequency reduction of between 2.5 and 15 %. It is difficult to measure precisely the observed frequency difference in Fig. 5, since it is of the same order of magnitude as the resolution of the 128 point FFT (3.9 Hz), but the effect of the orthodromic response could at least in part explain this discrepancy.

Frequency components of the phase-locked response

Using the stimulus-locked power method, we were able to analyse the frequency distribution of the phase-locked response in the LFP to PT stimulation. The most pronounced phase-locked effects were in the same frequency range, 15–30 Hz, which dominates the natural on-going LFP oscillations during the hold period of the task. In addition, we also found a phase-locked component in the cortical LFP at around 10 Hz. Single PTNs do not show phase locking with the LFP at these low frequencies (Pinches *et al.* 1999) and therefore the effects observed here may result from a separate neuronal circuit not incorporating PTNs. Interestingly, and in contrast to the beta band, we found no response at this 10 Hz frequency in the muscle EMG activity. A 10 Hz rhythm has also been observed over central cortical areas in human subjects using EEG and MEG techniques (Salmelin & Hari, 1994; Niedermeyer, 1997). However, no coherence with EMG is observed in this frequency band (Conway *et al.* 1995; Kilner *et al.* 2000), which is consistent with our finding of no phase-locked muscle activity at low frequencies. In addition, source localisation (Salenius *et al.* 1997) shows that the 10 and 20 Hz components arise from different cortical sources. This would also suggest that the circuits generating this lower frequency are distinct from those responsible for the 15–30 Hz frequencies. However, the phase-locked LFP response suggests that PT stimulation can result, directly or indirectly, in excitation of these circuits.

Finally, in some sessions a significant phase-locked response was observed at 40 Hz (Fig. 5*A*). Because this effect was small, we cannot rule out the possibility that it represents a harmonic of the lower frequencies. However, it is interesting to note that a 40 Hz oscillation, the 'Piper rhythm', can sometimes be observed in human motor cortex (Brown *et al.* 1998) and in the synchronous oscillation of motor cortex neurones (Baker *et al.* 2001).

Task dependence of oscillations

A number of studies have reported relationships between motor tasks and 15–30 Hz oscillations recorded in LFP, EEG or MEG (Sanes & Donoghue, 1993; Conway *et al.* 1995; MacKay & Mendonca, 1995; Baker *et al.* 1997; Kilner *et al.* 2000; see MacKay, 1997 for review). In all cases, beta activity was strongly suppressed during movement. Additionally in this study, we found that the oscillatory response to stimuli delivered during movement was much less pronounced than that during the hold period. Our hypothesis of delayed inhibitory feedback acting on PTNs provides a possible explanation of this phenomenon. During movements, PTNs typically fire at much higher rates than 15–30 Hz (Evarts, 1968; Lemon *et al.* 1986; Maier *et al.* 1993). Under these conditions, feedback would be modulated at these higher frequencies, no longer comparable to the 10–30 ms time course of the delayed inhibition. Thus, whilst this inhibitory feedback may still produce synchrony between PTNs during movement (Baker *et al.* 2001), it would no longer enforce a 15–30 Hz oscillation.

Conclusions

We have found a significant phase-locked response to PT stimulation in LFP, single-unit and EMG activity. This occurred principally in the 15–30 Hz frequency range and represents a resetting of the phase of beta band oscillations. Since oscillation is evident in PTN discharge, and PTN activity can reset these same rhythms, we conclude that PTNs are involved in the generation of the 15–30 Hz oscillations. This further emphasises a role for oscillations during particular phases of sensorimotor tasks, and is consistent with the speculation that this oscillatory activity helps to maintain the 'motor set' during periods of steady gripping behaviour.

Downloaded from jp.physoc.org by on March 23, 2008

REFERENCES

Abeles, M. (1982). Quantification, smoothing and confidence limits for single-units' histograms. *Journal of Neuroscience Methods* **5**, 317–325.

Abeles, M. (1991). *Corticonics*. Cambridge University Press, Cambridge, UK.

Ahmed, B. (2000). Low frequency damped oscillations of cat visual cortical neurones. *Neuroreport* **11**, 1243–1247.

Baker, S. N., Jackson, A., Spinks, R. & Lemon, R. N. (2001). Synchronization in monkey motor cortex during a precision grip task I. Task-dependent modulation in single-unit synchrony. *Journal of Neurophysiology* **85**, 869–885.

Baker, S. N., Olivier, E. & Lemon, R. N. (1997). Coherent oscillations in monkey motor cortex and hand muscle EMG show task dependent modulation. *Journal of Physiology* **501**, 225–241.

Baker, S. N., Olivier, E. & Lemon, R. N. (1998). An investigation of the intrinsic circuitry of the motor cortex of the monkey using intra-cortical microstimulation. *Experimental Brain Research* **123**, 397–411.

Baker, S. N., Philbin, N., Spinks, R., Pinches, E. M., Pauluis, Q., McManus, D., Lemon, R. N. & Wolpert, D. M. (1999). Multiple single unit recording in the cortex of monkeys using independently moveable microelectrodes. *Journal of Neuroscience Methods* **94**, 5–17.

Britton, T. C., Thompson, P. D., Day, B. L., Rothwell, J. C., Findley, L. J. & Marsden, C. D. (1993). Modulation of postural wrist tremors by magnetic stimulation of the motor cortex in patients with Parkinson's disease or essential tremor and in normal subjects mimicking tremor. *Annals of Neurology* **33**, 473–479.

Brown, P., Salenius, S., Rothwell, J. C. & Hari, R. (1998). Cortical correlate of the piper rhythm in humans. *Journal of Neurophysiology* **80**, 2911–2917.

Buys, E. J., Lemon, R. N., Mantel, G. W. H. & Muir, R. B. (1986). Selective facilitation of different hand muscles by single corticospinal neurones in the conscious monkey. *Journal of Physiology* **381**, 529–549.

Conway, B. A., Halliday, D. M., Shahani, U., Maas, P., Weir, A. L. & Rosenberg, J. R. (1995). Synchronization between motor cortex and spinal motoneuronal pool during the performance of a maintained motor task in man. *Journal of Physiology* **489**, 917–924.

DeFelipe, J., Hendry, S. H., Jones, E. G. & Schemechel, D. (1985). Variability in the terminations of GABAergic chandelier cell axons on initial segments of pyramidal cell axons in the monkey sensory-motor cortex. *Journal of Comparative Neurology* **231**, 364–384.

Evarts, E. V. (1968). Relation of pyramidal tract activity to force exerted during voluntary movement. *Journal of Neurophysiology* **31**, 14–27.

Feldman, J. L., McCrimmon, D. R. & Speck, D. F. (1984). Effect of synchronous activation of medullary inspiratory bulbospinal neurones on phrenic nerve discharge in cat. *Journal of Physiology* **347**, 241–254.

Ghosh, S. & Porter, R. (1988). Morphology of pyramidal neurones in monkey motor cortex and the synaptic actions of their intracortical axon collaterals. *Journal of Physiology* **400**, 593–615.

Gross, J., Tass, P. A., Salenius, S., Hari, R., Freund, H.-J. & Schnitzler, A. (2000). Cortico-muscular synchronization during isometric muscle contraction in humans as revealed by magnetoencephalography. *Journal of Physiology* **527**, 623–631.

Halliday, D. M., Conway, B. A., Farmer, S. F. & Rosenberg, J. R. (1998). Using electroencephalography to study functional coupling between cortical activity and electromyograms during voluntary contractions in humans. *Neuroscience Letters* **241**, 5–8.

Hari, R. & Salenius, S. (1999). Rhythmical corticomotor communication. *Neuroreport* **10**, R1–10.

Holdefer, R. N., Houk, J. C. & Miller, L. E. (1999). Reciprocal projections between cerebellum and motor cortex demonstrated at the single neuron level in the awake monkey. *Society of Neuroscience Abstracts* **25**, 914.

Holdefer, R. N., Miller, L. E., Chen, L. I. & Houk, J. C. (2000). Functional connectivity between cerebellum and primary motor cortex in the awake monkey. *Journal of Neurophysiology* **84**, 585–590.

Huntley, G. W. & Jones, E. G. (1991). Relationship of intrinsic connections to forelimb movement representations in monkey motor cortex: A correlative anatomic and physiological study. *Journal of Neurophysiology* **66**, 390–413.

Jackson, A., Freeman, T. C. B., Spinks, R. L., Wolpert, D. M. & Lemon, R. N. (2000). Effects of corticospinal activation on 15–35 Hz oscillatory activity in macaque motor cortex. *European Journal of Neuroscience* **12**, 506.

Jervis, B. W., Nichols, M. J., Johnson, T. E., Allen, E. & Hudson, N. R. (1983). A fundamental investigation of the composition of auditory evoked potentials. *IEEE Transactions in Biomedical Engineering* **30**, 43–50.

Kalcher, J. & Pfurtscheller, G. (1995). Discrimination between phase-locked and non-phase-locked event-related EEG activity. *Electroencephalography and Clinical Neurophysiology* **94**, 381–384.

Kang, Y., Endo, K. & Araki, T. (1991). Differential connections by intracortical axon collaterals among pyramidal tract cells in the cat motor cortex. *Journal of Physiology* **435**, 243–256.

Kilner, J. M., Baker, S. N., Salenius, S., Hari, R. & Lemon, R. N. (2000). Human cortical muscle coherence is directly related to specific motor parameters. *Journal of Neuroscience* **20**, 8838–8845.

Kilner, J. M., Baker, S. N., Salenius, S., Jousmaki, V., Hari, R. & Lemon, R. N. (1999). Task-dependent modulation of 15–30 Hz coherence between rectified EMGs from human hand and forearm muscles. *Journal of Physiology* **516**, 559–570.

Kisvarday, Z. F., Gulyas, A., Beroukas, D., North, J. B., Chubb, I. W. & Somogyi, P. (1990). Synapses, axonal and dendritic patterns of GABA-immunoreactive neurons in human cerebral cortex. *Brain* **113**, 793–812.

Kujirai, T., Caramia, M. D., Rothwell, J. C., Day, B. L., Thompson, P. D., Ferbert, A., Wroe, S., Asselman, P. & Marsden, C. D. (1993). Corticocortical inhibition in human motor cortex. *Journal of Physiology* **471**, 501–519.

Kuypers, H. G. J. M. (1981). Anatomy of the descending pathways. In *Handbook of Physiology*, section 1, *The Nervous System*, vol. II, ed. Brookhart, J. M. & Mountcastle, V. B., pp. 597–666. American Physiological Society, Bethesda, MD, USA.

Landry, P., Labelle, A. & Deschenes, M. (1980). Intracortical distribution of axonal collaterals of pyramidal tract cells in the cat motor cortex. *Brain Research* **191**, 327–336.

Lemon, R. N. (1984). Methods for neuronal recording in conscious animals. In *IBRO Handbook Series: Methods in Neurosciences 4*, ed. Smith, A. D., pp. 1–162. Wiley, London, UK.

Lemon, R. N. (1993). Cortical control of the primate hand. *Experimental Physiology* **78**, 263–301.

Lemon, R. N., Mantel, G. W. H. & Muir, R. B. (1986). Corticospinal facilitation of hand muscles during voluntary movement in the conscious monkey. *Journal of Physiology* **381**, 497–527.

Downloaded from jp.physoc.org by on March 23, 2008

Lytton, W. W. & Sejnowski, T. J. (1991). Simulations of cortical pyramidal neurons synchronised by inhibitory interneurons. *Journal of Neurophysiology* **66**, 1059–1079.

MacKay, W. A. (1997). Synchronised neuronal oscillations and their role in motor processes. *Trends in Cognitive Sciences* **1**, 176–183.

MacKay, W. A. & Mendonca, A. J. (1995). Field potential bursts in parietal cortex before and during reach. *Brain Research* **704**, 167–174.

Maier, M., Bennett, K. M. B., Hepp-Reymond, M.-C. & Lemon, R. N. (1993). Contribution of the monkey cortico-motoneuronal system to the control of force in precision grip. *Journal of Neurophysiology* **69**, 772–785.

Marsden, J. F., Ashby, P., Limousin-Dowsey, P., Rothwell, J. C. & Brown, P. (2000). Coherence between cerebellar thalamus, cortex and muscle in man. *Brain* **123**, 1459–1470.

Miller, L. E., Van Kan, P. L. E., Sinkjaer, T., Andersen, T., Harris, G. D. & Houk, J. C. (1993). Correlation of primate red nucleus discharge with muscle activity during free-form arm movements. *Journal of Physiology* **469**, 213–243.

Mills, K. R. & Schubert, M. (1995). Short term synchronisation of human motor units and their responses to transcranial magnetic stimulation. *Journal of Physiology* **483**, 511–523.

Mima, T., Steger, J., Schulman, A. E., Gerloff, C. & Hallet, M. (2000). Electroencephalographic measurement of motor cortex control of muscle activity in humans. *Clinical Neurophysiology* **111**, 326–337.

Murthy, V. N. & Fetz, E. E. (1992). Coherent 25- to 35-Hz oscillations in the sensorimotor cortex of awake behaving monkeys. *Proceedings of the National Academy of Sciences of the USA* **89**, 5670–5674.

Murthy, V. N. & Fetz, E. E. (1996). Oscillatory activity in sensorimotor cortex of awake monkeys: synchronization of local field potentials and relation to behavior. *Journal of Neurophysiology* **76**, 3949–3967.

Niedermeyer, E. (1997). Alpha rhythms as physiological and abnormal phenomena. *International Journal of Psychophysiology* **26**, 31–49.

Pauluis, Q., Baker, S. N. & Olivier, E. (1999). Emergent oscillations in a realistic network: the role of inhibition and the effect of the spatiotemporal distribution of the input. *Journal of Computational Neuroscience* **6**, 27–48.

Pellerin, J.-P. & Lamarre, Y. (1997). Local field potential oscillations in primate cerebellar cortex during voluntary movement. *Journal of Neurophysiology* **78**, 3502–3507.

Perkel, D. H., Schulman, J. H., Bullock, T. H., Moore, G. P. & Segundo, J. P. (1964). Pacemaker neurons: effects of regularly spaced synaptic input. *Science* **145**, 61–63.

Pfurtscheller, G. & Lopes da Silva, F. H. (1999). Event-related EEG/MEG synchronisation and desynchronisation: basic principles. *Clinical Neurophysiology* **110**, 1842–1857.

Pinches, E. M., Baker, S. N. & Lemon, R. N. (1997). Quantitative assessment of phase locking in discharge of identified pyramidal tract neurones during 25 Hz oscillations in monkey motor cortex. *Journal of Physiology* **501**, 36*P*.

Pinches, E. M., Baker, S. N. & Lemon, R. N. (1999). Frequency domain analysis of the synchrony between local field potentials and output neurones recorded in macaque motor cortex during precision grip. *Journal of Physiology* **515**, 156*P*.

Piper, H. (1907). Über den willkurlichen Muskeletanus. *Pflügers Archiv Gesamte Physiol Menschen und Tieren* **199**, 301–338.

Pohja, M., Salenius, S., Roine, R. O. & Hari, R. (2000). Cerebellar infarct decreases rhythmic activity outflow from the motor cortex. *European Journal of Neuroscience* **12**, 199.

Porter, R. & Lemon, R. N. (1993). *Corticospinal Function and Voluntary Movement.* Clarendon Press, Oxford, UK.

Renaud, L. P. & Kelly, J. S. (1974*a*). Identification of possible inhibitory neurons in the pericruciate cortex of the cat. *Brain Research* **79**, 9–28.

Renaud, L. P. & Kelly, J. S. (1974*b*). Simultaneous recordings from pericruciate pyramidal tract and non-pyramidal tract neurons; response to stimulation of inhibitory pathways. *Brain Research* **79**, 29–44.

Salenius, S., Portin, K., Kajola, M., Salmelin, R. & Hari, R. (1997). Cortical control of human motoneuron firing during isometric contraction. *Journal of Neurophysiology* **77**, 3401–3405.

Salmelin, R. & Hari, R. (1994). Spatiotemporal characteristics of sensorimotor neuromagnetic rhythms related to thumb movement. *Neuroscience* **60**, 537–550.

Sanes, J. N. & Donoghue, J. P. (1993). Oscillations in local field potentials of the primate motor cortex during voluntary movement. *Proceedings of the National Academy of Sciences of the USA* **90**, 4470–4474.

Sayers, B. McA. & Beagley, H. A. (1974). Objective evaluation of auditory evoked EEG responses. *Nature* **251**, 608–609.

Snider, R. S. & Lee, J. C. (1961). *A Stereotaxic Atlas of the Monkey Brain* (*Macaca mulatta*). University of Chicago Press, Chicago, IL, USA.

Staras, K., Chang, H. S. & Gilbey, M. (2001). Resetting of sympathetic rhythm by somatic afferents causes post-reflex coordination of sympathetic activity in rat. *Journal of Physiology* **533**, 537–545.

Steriade, M. (1999). Coherent oscillations and short-term plasticity in corticothalamic networks. *Trends in Neurosciences* **22**, 337–345.

Tallon-Baudry, C., Bertrand, O., Delpuech, C. & Pernier, J. (1996). Stimulus specificity of phase-locked and non-phase-locked 40 Hz visual responses in human. *Journal of Neuroscience* **16**, 4240–4249.

Tass, P. A. (1999). *Phase Resetting in Medicine and Biology*. Springer-Verlag, Berlin, Germany.

Thomson, A. M. & Deuchars, J. (1997). Synaptic interactions in neocortical local circuits: dual intracellular recordings in vitro. *Cerebral Cortex* **7**, 510–522.

Thomson, A. M., West, D. C. & Deuchars, J. (1995). Properties of single axon excitatory postsynaptic potentials elicited in spiny interneurons by action potentials in pyramidal neurons in slices of rat neocortex. *Neuroscience* **69**, 727–738.

Thomson, A. M., West, D. C., Hahn, J. & Deuchars, J. (1996). Single axon IPSPs elicited in pyramidal cells by three classes of interneurones in slices of rat neocortex. *Journal of Physiology* **496**, 81–102.

Ugolini, G. & Kuypers, H. G. J. M. (1986). Collaterals of corticospinal and pyramid fibres to the pontine grey demonstrated by a new application of the fluorescent fibre labelling technique. *Brain Research* **365**, 211–227.

Wagener, D. S. & Colebatch, J. G. (1996). Voluntary rhythmical movement is reset by stimulating the motor cortex. *Experimental Brain Research* **111**, 113–120.

Whittington, M. A., Traub, R. D. & Jefferys, J. G. (1995). Synchronised oscillations in interneuron networks driven by metabotropic glutamate receptor activation. *Nature* **373**, 563–564.

Whittington, M. A., Traub, R. D., Kopell, N., Ermentrout, B. & Buhl, E. H. (2000). Inhibition-based rhythms: experimental and mathematical observations on network dynamics. *International Journal of Psychophysiology* **38**, 315–336.

Downloaded from jp.physoc.org by on March 23, 2008

Acknowledgements
The authors thank Stuart Baker, Thomas Brochier, Chris Seers and Helen Lewis for their assistance. This work was funded by the Medical Research Council, The Wellcome Trust and the Human Frontiers Science Program.

Author's present address
T. C. B. Freeman: Institute of Neuroinformatics, ETH, Zurich Winterthurerstrasse 190, CH-8057, Switzerland.

Downloaded from jp.physoc.org by on March 23, 2008

Rhythm generation in monkey motor cortex explored using pyramidal tract stimulation

A. Jackson, R. L. Spinks, T. C. B. Freeman, D. M. Wolpert and R. N. Lemon

J. Physiol. 2002;541;685-699; originally published online Apr 19, 2002;

DOI: 10.1113/jphysiol.2001.015099

This information is current as of March 23, 2008

Updated Information & Services	including high-resolution figures, can be found at: http://jp.physoc.org/cgi/content/full/541/3/685
Permissions & Licensing	Information about reproducing this article in parts (figures, tables) or in its entirety can be found online at: http://jp.physoc.org/misc/Permissions.shtml
Reprints	Information about ordering reprints can be found online: http://jp.physoc.org/misc/reprints.shtml

Downloaded from jp.physoc.org by on March 23, 2008